CHANGE DETECTION APPROACH TO SAR AND OPTICAL IMAGE INTEGRATION

Yu ZENG [a,b], Jixian ZHANG [b], J.L.VAN GENDEREN [c]

[a] Shandong University of Science and Technology, Qingdao, Shandong Province, 266510, P.R.China
[b] Chinese Academy of Surveying and Mapping, Beijing, 100039, P.R.China, zengyu@casm.ac.cn
[c] International Institute for Aerospace Survey and Earth Sciences (ITC),
P.O. Box 6, 7500 AA Enschede, The Netherlands

Commission VII, WG VII/6

KEY WORDS: Environmental Monitoring, Change Detection, Fusion, Land Use, Land Cover, SPOT5, RADARSAT

ABSTRACT:

In order to overcome the insufficiency of single remote sensing data source during information extraction, to make use of the complementary characteristics of SAR data and optical imagery, and to facilitate better monitoring and evaluation of resources and ecological environment, this paper develops the idea and presents the approach to land use/cover change detection by different temporal SAR and optical image integration. Aiming at the different imaging mechanisms and information characteristics of optical imagery and SAR data, this paper employs the object-oriented image analysis technique for high accuracy information extraction from high-resolution optical imagery; it proposes a multi-scale and multi-texture feature fusion method based on SVM for information extraction from single-band and single-polarization SAR data by employing the multi-scale textural analysis technique and the fractal analysis technique; it then integrates individually extracted information of different temporal for change information extraction by applying a series of decision rules; it also develops the method for analysis and evaluation of uncertainty of the change detection result at the scale of pixels using the extended probability vector. Data adopted in this research are different temporal SPOT5 image and Radarsat-1 SAR data. Experimental results prove the correctness, reliability and effectiveness of the methods proposed in this paper.

1. INTRODUCTION

Timely and accurate change detection of Earth's surface features is extremely important for understanding relationships and interactions between human and natural phenomena in order to effectively manage and use resources as well as to promote better decision making. Because of the advantages of repetitive data acquisition, its synoptic view, and digital format suitable for computer processing, remote sensing data, such as AVHRR, Landsat TM/ETM$^+$, SPOT, IKONOS, SAR and aerial photographs, have become the major data sources for different change detection applications during the past decades.

Optical sensors acquire the reflected energy from sunlight reaching the ground in the visible and near-infrared spectrum. While the multi-spectral data presents the rich spectral information of the observed objects, the panchromatic data which is often available with a higher resolution than multi-spectral data shows detailed geometric information of the objects. These features make optical imagery relatively easier for interpretation and become the main remote sensing data source for change detection. However, due to the limitation of data acquisition, such as the impact of clouds, fog, or smoke on optical sensors, sometimes, it is difficult to obtain the same sensor optical images that meet the temporal requirement. Different from optical sensors, a SAR sensor has the all-weather capability. Factors which influence the intensity of radar returns determine that SAR data can present rich structural and texture information, and is sensitive to water body, vegetation, and built-up areas. However, due to the limited band numbers and polarization modes, as well as the affects caused by speckle noises, slant-range imaging, foreshortening, layover, and shadows, SAR data is relatively difficult for interpretation compared with the optical imagery.

In order to overcome the insufficiency of single remote sensing data source during information extraction, to make use of the complementary characteristics of SAR data and optical imagery, and to facilitate better monitoring and evaluation of resources and ecological environment, this paper develops the idea and presents the approach to land use/cover change detection by different temporal SAR and optical image integration. Test site of this research is located at Jinnan district, Tianjin, China. Data adopted are SPOT5 Pan/XS image acquired on October 16, 2004 and SGF F3 Radarsat-1 SAR data acquired on October 19, 2005 with the spatial resolution 6.25m. The rest of the paper is organized as follows. Section 2 gives an overview on the methodology of this research. Section 3 describes the experimental results and their analysis and conclusions are drawn in Section 4.

2. METHODS

2.1 Object-oriented Image Analysis Technique

Different from pixel-based image classification approach, object-oriented image classification operates on objects instead of single pixels. These objects consist of many pixels that have been grouped together in a certain way by image segmentation, and each object is homogeneous and non-intersecting with the others. Object-oriented image analysis technique uses shape, size, textural, contextual information as well as spectral information to perform information extraction at the level of objects. While high spatial resolution remote sensing provides more information than coarse resolution imagery for detailed observation on ground objects, single pixels no longer capture the characteristics of classification targets, and the increase in intra-class spectral variability causes a reduction of statistical separability between classes with traditional pixel-based classification approaches. Consequently, classification accuracy is reduced, and the classification results show a salt-and-pepper effect. Because of the characteristics of high resolution imagery, lots of object-oriented image analysis was done and research results prove the effectiveness of object-oriented image analysis for information extraction from high spatial resolution imagery (Baatz and Schape,1999; Blaschke et al., 2000; eCognition, 2002; Benz et al., 2004; Volker, 2004; Yan G et al., 2006).

An object-based approach to image analysis is composed of four steps, which are multi-resolution segmentation to generate objects resembling ground objects closely and to create object hierarchy which allows a simultaneous representing of image features of various scale and establishes a network allowing relations between objects to be utilized, image object feature extraction and parameter assessment which help to find useful features and ways to separate classes, classification which uses iterative steps to classify image objects, as well as accuracy analysis and evaluation. In this research, object-oriented fuzzy classification to optical imagery was performed in Definiens 5.0, which is an object-based processing software from Definiens Imaging GmbH.

2.2 Information Extraction from SAR Imagery Based on Textural Features

Texture, a representation of the spatial relationship of grey-levels in an image, is an important characteristic for the automated or semi-automated interpretation of digital imagery. SAR image is the representation of backward scattering characteristics of ground objects to radar waves. If the ground objects have same or similar backward scattering values, it is difficult to get them separated, especially in the single band and single polarization SAR imagery. In addition, because of the influence of speckle noises, it is hard to distinguish ground objects only by intensity values. Textural information should be utilized (Guo et al., 2000).

Nowadays, different methods have been proposed for analysis of image texture, and there is no general agreement on an overall best analysis method, which outperforms all the others on various tasks. In this research, we propose a multi-scale and multi-texture feature fusion method based on SVM (Support Vector Machine) for information extraction from single-band and single-polarization SAR data by employing the multi-scale textural analysis technique and the fractal analysis technique. The method makes use of the ability of GLCM (Grey Level Co-occurrence Matrix) which uses spatial correlated characteristic of grey values for texture description, takes the multi-scale features of ground objects into account, and incorporates multi-fractal features which have the great capability in description of complex spatial structure information and detailed texture features; on the basis of SVM and by using feature-level image fusion technique, it integrates seven textural features to realize the land use/cover classification of SAR imagery. SVM is introduced in this research because it is established on the basis of statistical learning theory, and has favourable classification performance in the feature space which is nonlinear, high-dimensional and has small samples. The seven-dimensional textural features are:

Feature 1: Correlation feature with the processing window size 11;
Feature 2: Standard Deviation feature with the processing window size 21;
Feature 3: Entropy feature with the processing window size 13;
Feature 4: Fractal dimension feature;
Feature 5-6: two multi-fractal features;
Feature 7: Second-order statistic lacunarity;
Where, the first three multi-scale GLCM features are obtained according to multi-scale textural analysis, which can be referred to Zeng et al.(2007a); the latter four features are based on fractal theory and are obtained according to fractal analysis. The calculation of fractal dimension feature can be referred to Zeng et al.(2007b).

Improving the interpretation accuracy of SAR data is the basis for change detection with optical imagery at the level of information processing.

2.3 Soft-decision Change Detection Based on Rules

On the basis of above research, the change information can be obtained by combining individually extracted information of different temporal. Aiming at the change overestimation caused by error propagation and the traditional hard-decision method for change detection, this research proposes a soft-decision method based on rules for change detection. In China, land use/cover change usually occurs at the urban fringe areas, and most land use/cover changes are the consequence of urban growth. In this instance, we can think that change to built-up area from other land use types is irreversible. With the rapid economy development and population growth, the emphases of land use change monitoring in China are urban expansion and decrease of plantation areas. Taking the characteristics of land use change at the urban fringe areas and the research focus into account, this method employs a series of logic rules in turn to evaluate the rationality of the detected changes. The logic rules are made according to the status of pixels which are changed or unchanged, land use change trajectories, as well as by taking the spatial features of detected changes which are shape, size and location into consideration.

Let Num denotes the number of detected changes. Land use types are presented as C_i. Here, C_1 = “built-up area”, C_2 = “water”, C_3 = “vegetation”, C_4 = “bare land”. The detected change trajectory is denoted as $T(C_i,...)$. Let N refers to “no change”, W refers to “wrong classification and applying masking”, and Y refers to “correctly detected changes”. These logic rules are:

Rule 1: $IF \quad Num = 0 \quad THEN \quad N$.
Rule 2: $IF \quad Num = 1 \quad AND \quad T(C_i, C_j) \quad (i \neq 1; i \neq j) \quad THEN \quad Y$.
Rule 3: $IF \quad Num = 1 \quad AND \quad T(C_1, C_j) \quad (j \neq 1) \quad THEN \quad W$.
Rule 4: River, lake, canal and its affiliated works are regarded as N.
Rule 5: Land use types in between large area of cultivated lands are regarded as N.
Rule 6: Isolated 3×3 detected change regions are regarded as W.

By employing these rules in turn to analyze the rationality of the detected changes, the unchanged areas, falsely detected changes, and possible changes can be separated. The change overestimation can be decreased and the change detection accuracy can be improved.

2.4 Uncertainty of Change Detection Result

Uncertainty, or error, exists from remote sensing data acquisition to each stage of data processing. Understanding the nature and spatial distribution of uncertainty during the process of change detection result analysis, can reduce the risk of wrong decision based on the uncertain data. Based on the classification results, there are several uncertainty propagation models of change detection such as the product rule-based approach, the certainty factor-based approach (Shi and Ehlers, 1996), and the probability entropy approach (Van der Wel et al., 1998; DE Bruin and Gorte, 2000). In this research, we extend the probability vector which is usually used for maximum likelihood classification to the object-oriented fuzzy classification and the multi-scale and multi-texture feature fusion classification based on SVM, then further analyze and evaluate uncertainty of the change detection result at the scale of pixels based on the probability entropy model, which is briefly described as below:

Different temporal image classification can be regarded as independent. In other words, the posterior probability vector of a pixel at time t2 is calculated irrespective of the class or feature vector at the previous time, t1. According to Shannon's information theory, entropy is calculated as

$$H = -\sum_{j=1}^{M}\sum_{i=1}^{M} P_{ij}\log_2(P_{ij})$$

$$= -\sum_{i=1}^{M} P(C_{i,T1}/X_{T1})\log_2(P(C_{i,T1}/X_{T1})) - \sum_{j=1}^{M} P(C_{j,T2}/X_{T2})\log_2(P(C_{j,T2}/X_{T2})) \quad (1)$$

Where,

$$P_{ij} = P(C_{i,T1}, C_{j,T2}/X_{T1}, X_{T2}) = P(C_{i,T1}/X_{T1})P(C_{j,T2}/X_{T2}),$$

M represents the number of classes. The range of H is from 0 to $\log_2(MM)$, which means uncertainty varies from absolute certain to absolute uncertain.

3. EXPERIMENTAL RESULTS AND ANALYSIS

3.1 Information Extraction from SPOT5 Image

Both SPOT5 2.5-meter panchromatic band and four 10-meter multi-spectral bands are used in the object-oriented fuzzy classification. The first level classes are built-up land, vegetation, water body and bare land. Where, built-up land consists of three subclasses which are building, building shadow and road; vegetation consists of four subclasses which are forest, grassland, cropland (including irrigated field and nonirrigated field), and vegetable plot (including vegetable greenhouse); water body consists of two subclasses which are river/canal and lake/pond. NDVI image is also produced as the additional band for classification. During the multi-resolution segmentation, the weight of SPOT5 panchromatic band and multi-spectral bands are assigned to one respectively. After several times of experiments, a network of three layers is constructed according to features of ground objects. The setting of parameters is given in Table 1.

Level	Scale	Color	Shape	Composition of shape	
				Smoothness	Compactness
Level 3	110	0.8	0.2	0.5	0.5
Level 2	90	0.9	0.1	0.4	0.6
Level 1	40	0.8	0.2	0.4	0.6

Table 1. Parameter setting for multi-resolution segmentation

After the object hierarchy has been established, the nearest neighbour classifier and the classifier of membership function are integrated to obtain spectral, textural, shape, positional and contextual information of image objects. Then, by establishing the classification rules to realize the effective separation to ground objects in the complex scene (Figure 1).

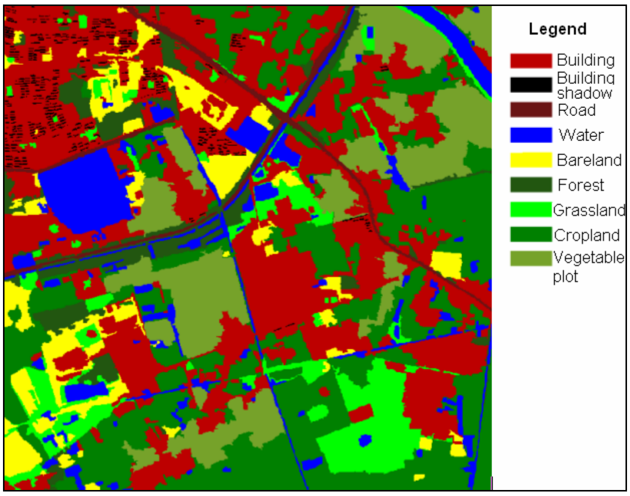

Figure 1. Fuzzy object-oriented classification result of the test site (partial)

From Table 2, it can be seen that for the second level classification, the overall accuracy is 88.53%, Kappa coefficient is 0.861; for the first level classification, the overall accuracy reaches to 90.19% and Kappa coefficient reaches to 0.872.

	Class	Producer's accuracy %	User's accuracy %	Overall accuracy %	Kappa coefficient
Level 2	Building	85.28	92.11	88.53	0.861
	building shadow	86.03	90.27		
	road	79.34	81.42		
	forest	83.00	71.18		
	grassland	84.47	73.65		
	cropland	90.91	84.43		
	vegetable plot	91.18	82.36		
	river/canal	79.16	76.02		
	lake/pond	92.56	86.72		
	bare land	80.81	85.75		
Level 1	built-up land	87.90	92.73	90.19	0.872
	bare land	80.81	85.75		
	vegetation	92.25	85.97		
	water body	90.90	84.48		

Table 2. Accuracy evaluation for the fuzzy object-oriented classification

High performance of information extraction from optical imagery is the basis for change detection with SAR data at the information processing level.

3.2 Information Extraction from Radarsat-1 SAR Image

Considering some of the fractals have the same fractal dimensions but have the different textures, on the basis of textural analysis using fractal dimensions, this research further introduces multi-fractal theory and the second-order statistic lacunarity as the effective supplements to fractal dimension for textural analysis. Samples of typical ground objects were extracted, then the multi-fractal q-D(q) curve and the lacunarity L-C(L) curve were plotted in order to quantitatively determine the optimum parameters for effective fractal features extraction (Figure 2,3). From Table 2 and Table 3, we can see that when q equals to 8 and -8, L equals to 2, there is good separability among ground objects, so they were selected as the effective parameters for feature extraction.

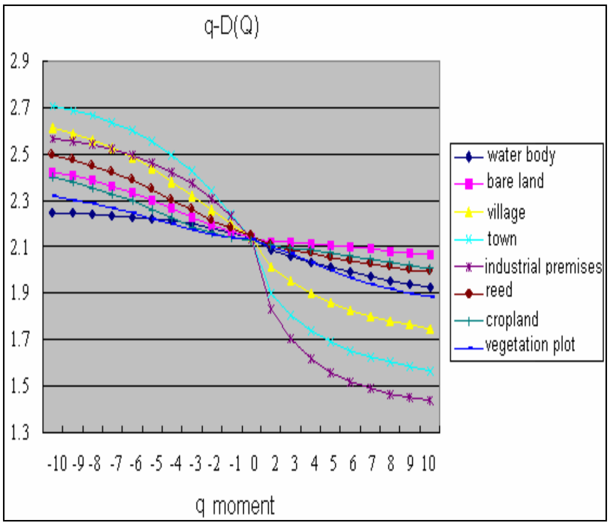

Figure 2. Multi-fractal q-D(q) curve of the typical ground objects

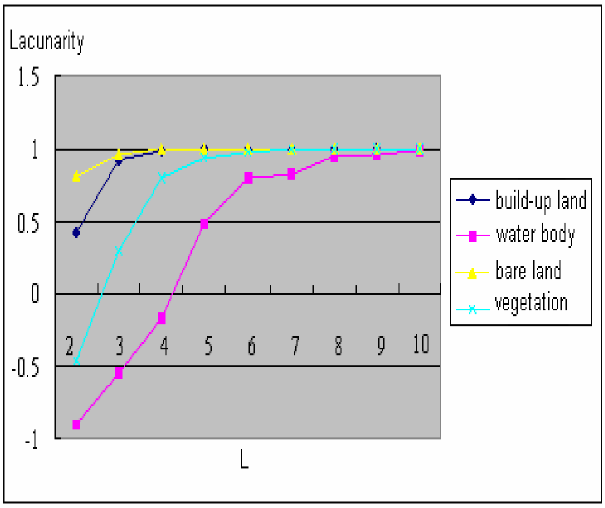

Figure 3. Lacunarity L-C(L) curve based on DBC method

Based on SVM, and using the seven multi-scale and multi-texture textural features mentioned in 2.2 as input, Radarsat-1 SAR image can be classified (Figure 4).

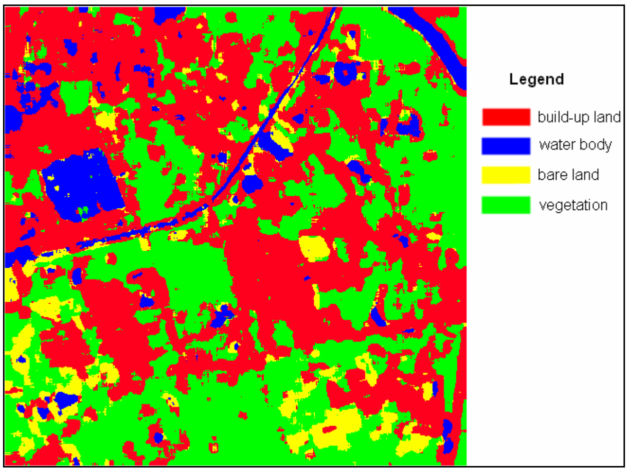

Figure 4. Classification result of SAR image based on multi-scale and multi-texture feature fusion and SVM (part of the test site)

In order to test the classification performance of different textural features, based on SVM, this research designed a classification scheme (Table 3). From Table 3 and Table 4, it can be seen that the fused seven features can reach better classification performance than any single or any other combination of the features and the improvement of the classification accuracy is significant.

Group No.	Feature for classification	Overall accuracy %	Kappa coefficient
1	multi-scale and multi-texture feature (Multi-scale GLCM+Three types of fractal features)	69.8926	0.4916
2	Multi-scale GLCM	67.2711	0.4680
3	Three types of fractal features (FD+multiFD+Lacu)	66.8600	0.4452
4	Multi-scale GLCM+FD	68.1001	0.4690
	Multi-scale GLCM+multiFD	68.2594	0.4700
	Multi-scale GLCM+Lacu	68.5601	0.4751
5	Multi-scale GLCM+FD+multiFD	68.5857	0.4789
	Multi-scale GLCM+FD+Lacu	69.4600	0.4803
	Multi-scale GLCM+multiFD+Lacu	69.4831	0.4889
6	SAR intensity image	54.4739	0.2395
	SAR backscattering coefficient image	45.9268	0.2139

Table 3. Classification accuracy analysis of SAR image based on multi-scale and multi-texture feature fusion and SVM

Z value	Group 1	Group 2	Group 3
Group 1			
Group 2	37.76787		
Group 3	57.63155	19.93228	

Table 4. Comparison of Z statistic

The classification performance between traditional maximum likelihood classification and SVM was also compared in this research. Using the same seven fused textural features as input, the classification accuracy is compared and Z statistic is given in Table 5. From Table 5, we can see that overall accuracy of SVM classification is higher than that obtained using MLC by 10%, Kappa coefficient is improved, and the Z statistic is 71.6227. It can be concluded that SVM is an effective classifier for textural features, and it can significantly improve the classification accuracy compared with the MLC classifier.

Classifier	Class	Producer's accuracy %	User's accuracy %	Overall accuracy %	Kappa coefficient
MLC	built-up land	45.57	72.34	59.1143	0.3816
	bare land	43.29	63.76		
	vegetation	64.56	52.52		
	water body	53.42	48.72		
SVM	built-up land	77.15	64.39	69.8926	0.4916
	bare land	60.76	66.61		
	vegetation	70.98	77.54		
	water body	50.49	53.23		
Z value	71.6227				

Table 5. Comparison of Z statistic for MLC and SVM

3.3 Change Detection Result and Uncertainty Analysis

By the direct post-classification comparison, the change detection result can be obtained (Figure 5). Where, the black represents no change, the green represents positive difference

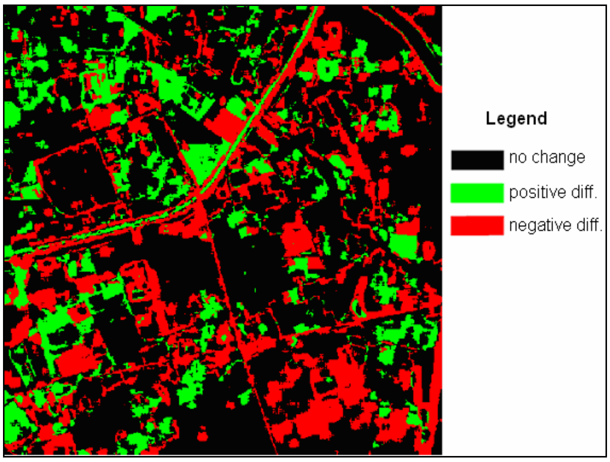

Figure 5. Change detection result of the test site based on the hard-decision (partial)

values and the red represents negative difference values (the classification code is: bare land 1, built-up land 2, vegetation 3 and water body 4). In order to effectively evaluate the change detection accuracy, special effort sampling was done and the number of samples was calculated according to multinomial distribution recommended by Khorram (Siamak Khorram et al., 1999). According to Table 6, the overall accuracy of the change detection result is 62.7%.

		Reference data		Sum in row
		unchanged	changed	
Classification data	unchanged	163	37	200
	changed	187	213	400
Sum in column		350	250	600

Table 6. Accuracy analysis for the hard-decision change detection

On the basis of the extended probability vector of the classification result with different temporal, and according to the probability entropy model of uncertainty propagation, the spatial distribution of uncertainty of change detection result at the scale of pixels can be obtained, which is shown in Figure 6. From this figure, we can see that the blacker area represents smaller uncertainty of the change detection result; usually, there exists higher uncertainty on the fringe of different land use/cover types.

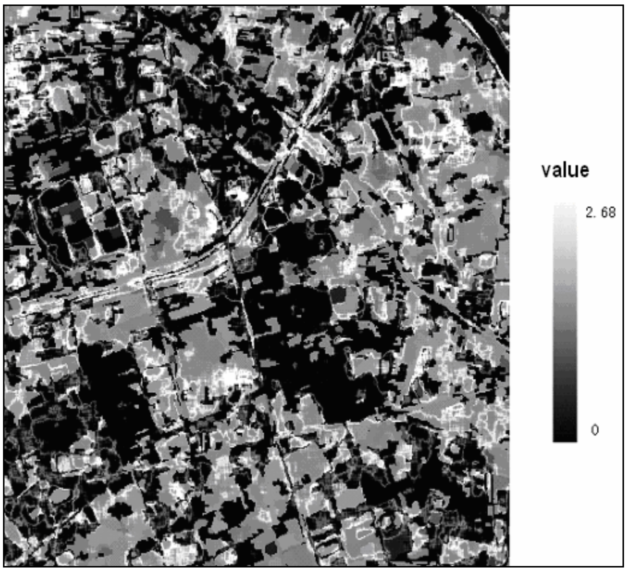

Figure 6. Spatial distribution of uncertainty of the change detection result represented by probability entropy

Interval of entropy (Δ)	0-0.4	0.4-0.8	0.8-1.2	1.2-1.6	1.6-2.0
Pixel percentage (%)	39.91	6.94	30.97	2.54	14.19
Accumulative percentage (%)	39.91	46.85	77.82	80.36	94.55
Interval of entropy (Δ)	2.0-2.4	2.4-2.8	2.8-3.2	3.2-3.6	3.6-4.0
Pixel percentage (%)	4.81	0.64	0.0	0.0	0.0
Accumulative percentage (%)	99.36	100.0	100.0	100.0	100.0

Table 7. Uncertainty of the change detection result

Separate the entropy value into ten intervals according to the range of entropy, then count the number of pixels falling in between each interval. From Table 7, it can be seen that nearly 95% pixels have the uncertainty less than 2.0. It means that although uncertainty increases during the process of error propagation, the change detection result by hard-decision still has the acceptable certainty level in this research.

Employ the soft-decision change detection method described in 2.3 for the further analysis (Figure 7). We can see that by executing the rules in turn, lots of false detected changes are eliminated, for example, after executing the rule 1-3, the area of detected changes decreased by 22.6%, and after executing the rule 4-6, the area of detected changes decreased by another 28.9%.

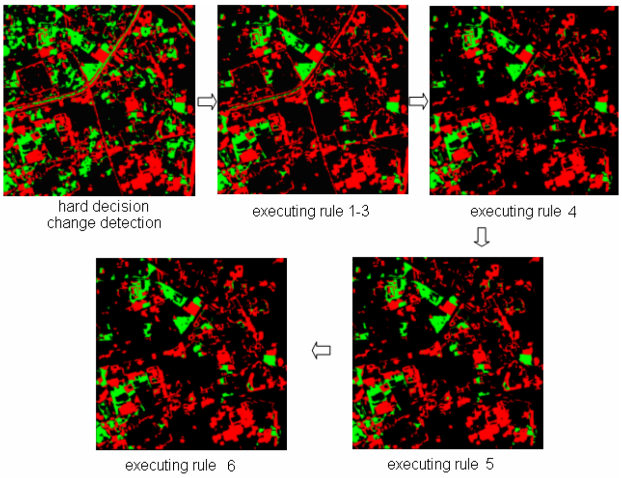

Figure 7. Soft-decision change detection based on rules

By applying the same accuracy analysis method applied to the hard-decision change detection result, from Table 8, it can be seen that the soft-decision analysis can generate improved change detection result, the omission error is 6.5%, the commission error is 15.3%; compared with Table 6, the overall accuracy is improved from 62.7% to 78.2%, and the commission error is reduced by half.

		Reference data		Sum in row
		unchanged	changed	
Classification data	unchanged	161	39	200
	changed	92	308	400
Sum in column		253	347	600

Table 8. Accuracy evaluation for the soft-decision change detection

2004 / 2005	vegetation	built-up land	bare land	water body
vegetation		0.0	0.0	0.39
built-up land	149.0		7.5	4.8
bare land	173.6	0.0		18.8
water body	7.8	0.0	0.0	

Table 9. Area change of the land use types of the test site (Area unit: hectare)

The statistic of the change of the area of each land use type in the research area (Table 9) shows that from October 2004 to October 2005, the main land use/cover changes are the decrease of vegetation, as well as the increase of the built-up land and the bare land. By further analyzing the classified result of the SPOT5 image acquired in 2004, we find out that in the trajectory of vegetation to built-up land, 20% of vegetation is cropland and 80% of vegetation is grassland. Because the study area is located at the downstream region of Haihe River, which belongs to the fluvial plain and marine plain, the annual mean relative humidity is high, and the case of vegetation changed to bare land usually occur when the parcel has been authorized to be used as built-up land but construction has not been done or just at the beginning of the construction. The circumstance of the decrease of vegetation, as well as the increase of the built-up land and the bare land well reflects the phenomenon and the trend of urban expansion and the occupation of the cropland and the unused land at the urban fringe areas.

4. CONCLUSIONS

Because of the different imaging mechanisms, optical imagery and SAR data has different and complementary image characteristics and information content. In order to overcome the insufficiency of single remote sensing data source during change detection, and to make use of the complementary characteristics of these two kinds of data source, this paper develops the idea and presents the approach to land use/cover change detection by different temporal SAR and optical image integration. Data adopted in this research are SPOT5 image and Radarsat-1 SAR data. With the successful launch of the high-resolution and polarized SAR data since the end of last year, such as Cosmo-SkyMed (Italy), TerraSAR-X (German) and Radarsat-2 (Canada), it provides us more choices for SAR data selection. With the abundant textural information and rich polarization information presented in these data, change detection accuracy will be improved considerablely.

REFERENCES

Baatz M and Schape A.1999.Object-oriented and multi-scale image analysis in semantic networks. *Proceedings of the 2nd international symposium on operationalization of remote sensing.*

Benz U C, et al. 2004. Multi-resolution, object-oriented fuzzy analysis of remote sensing data for gis-ready information. *ISPRS Journal of Photogrammetry and Remote Sensing*, No.58, pp.239-258.

Blaschke T, et al., 2000.Object-oriented image processing in an integrated GIS/remote sensing environment and perspectives for environmental applications. *Environmental Information for Planning*, Metropilis-Verlag, pp.555-570.

DE Bruin S. and Gorte B. G. H. 2000. Probabilistic image classification using geological map units applied to land-cover change detection. *International Journal of Remote Sensing,*Vol.21, No.12, pp.2389-2402.

eCognition 4.0 User Guide.2002. Definiens Image GmbH. German.

Guo Huadong. et al., 2000. Theories and applications of Radar systems for Earth observation. *Beijing: Science Publisher*.

Siamak Khorram et al.1999. Accuracy assessment of remote sensing-derived change detection. Published by American Socitety for Phorogrammetry and Remote Sensing, Maryland, USA.

Shi W Z and Ehlers M.1996. Determining uncertainties and their propagation in dynamic change detection based on classified remotely-sensed images. *International Journal of Remote Sensing*, Vol. 17, No. 14, pp.2729-2741.

Van der Wel, F. J. M., Van der Gaag, L. C., and Gorte, B. G. H., 1998. Visual exploration of uncertainty in remote sensing classification. *Computers and Geosciences*, 24, pp.335-343.

Volker W. 2004. Object-based classification of remote sensing data for change detection. *ISPRS Journal of Photogrammetry and Remote Sensing*, No.58, pp.225-238.

Yan Gao. et al., 2006. Comparison of pixel-based and object-oriented image classification approaches - a case study in a coal fire area, Wuda, Inner Mongolia, China. *International Journal of Remote Sensing*, Vol. 27, No. 18, pp.4039 - 4055.

Zeng Yu. et al., 2007a. Multi-scale SAR land use/land cover classification based on co-occurrence probabilities. "Mapping without the Sun" —Techniques and Applications of Optical and SAR Imagery Fusion, 25-27 September 2007, Chengdu, China. (*The International Archives of the Photogrammetry, Remote Sensing and Spatial Information Sciences*, Vol XXXVI, Part 7/C54, pp39-42)

Zeng Yu. et al., 2007b. Fractal characteristics of very high resolution satellite imagery. *Proceedings of IGARSS (IEEE International Geoscience and Remote Sensing Symposium) 2007*, July 23 - 27, Barcelona, Spain.